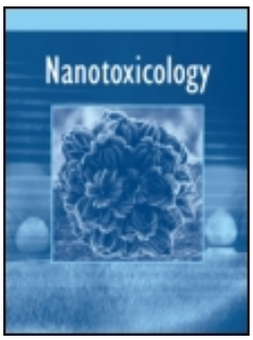

Nanotoxicology

ISSN: 1743-5390 (Print) 1743-5404 (Online) Journal homepage: https://www.tandfonline.com/loi/inan20

Preparation and properties of biocompatible PS-PEG/calcium phosphate nanospheres

Qi Wang, Peifeng Liu, Ying Sun, Tao Gong, Mingjie Zhu, Xun Sun, Zhirong Zhang & Yourong Duan

To cite this article: Qi Wang, Peifeng Liu, Ying Sun, Tao Gong, Mingjie Zhu, Xun Sun, Zhirong Zhang & Yourong Duan (2015) Preparation and properties of biocompatible PS-PEG/calcium phosphate nanospheres, Nanotoxicology, 9:2, 190-200, DOI: 10.3109/17435390.2014.911381

To link to this article: https://doi.org/10.3109/17435390.2014.911381

Published online: 30 Apr 2014.

http://informahealthcare.com/nan
ISSN: 1743-5390 (print), 1743-5404 (electronic)

Nanotoxicology

Nanotoxicology, 2015; 9(2): 190–200
 DOI: 10.3109/17435390.2014.911381

informa
healthcare

ORIGINAL ARTICLE

Preparation and properties of biocompatible PS-PEG/calcium phosphate nanospheres

Qi Wang[1,2]*, Peifeng Liu[1]*, Ying Sun[1], Tao Gong[2], Mingjie Zhu[1], Xun Sun[2], Zhirong Zhang[2], and Yourong Duan[1]

[1]State Key Laboratory of Oncogenes and Related Genes, Shanghai Cancer Institute, Renji Hospital, School of Medicine, Shanghai Jiao Tong University, Shanghai, China and [2]Key Laboratory of Drug Targeting and Novel Drug Delivery Systems, Ministry of Education, West China School of Pharmacy, Sichuan University, Chengdu, Sichuan, China

Abstract

A facile room-temperature method was used to prepare phosphatidylserine (PS)-poly(ethylene glycol) (PEG)/calcium phosphate (CaP) nanospheres (PS-poly(ethylene glycol) methyl ether/CaP nanospheres). Transmission electron microscopy (TEM) results confirmed that the PS-PEG/CaP porous nanospheres were spherical with a diameter of 8–12 nm. X-ray and thermo-gravimetric analysis (TGA) results also confirmed that the PS-PEG micelle was packed in the CaP shell. PS-PEG/CaP nanospheres exhibited little effect on the hemolysis, coagulation characteristics of blood and inflammatory response, demonstrating a negligible cytotoxicity response in LO_2 liver cells. Experiments performed in zebrafish demonstrated that the PS-PEG/CaP nanospheres had a long circulatory residence time and did not induce apoptosis in zebrafish. Taken together, these results suggest that the PS-PEG/CaP nanospheres have great potential to be used as a drug carrier.

Keywords

Biocompatible, biodistribution, cytotoxicity, drug carrier, nanospheres

History

Received 6 November 2013
Revised 13 January 2014
Accepted 6 March 2014
Published online 30 April 2014

Introduction

Calcium phosphate (CaP) cements were discovered in the 1980s (Bleek & Taubert, 2013; Ng et al., 2010; Olton et al., 2011). Since then, CaP precipitation formulations have been developed that fulfill the specific requirements for use in these applications, such as the delivery carriers of antibiotics, proteins, growth factors and anti-cancer drugs (Chow & Takagi, 2001; Shen et al., 2012). However, the disadvantages of CaP precipitation, including the uncontrollable rapid growth of CaP particles, results in bulk precipitation and a heterogeneous size distribution, which induces a low encapsulation efficiency and a large deviation in its drug release properties. These characteristics result in poor reproducibility and a low treatment effect (Cai & Yao, 2010), which greatly limits its further application.

To overcome these deficiencies, it is necessary to prevent the rapid growth of CaP particles and to avoid the formation of large-sized precipitates. For this, micro-emulsion and emulsion approaches have been used to modulate the size of CaP nanoparticles (Bisht et al., 2005; Fujiwara et al., 2008), and polymer-assisted methods have been developed to obtain nanoparticles of a well-defined size and morphology (Wang et al., 2010a; Wu et al., 2013; Mukesh et al., 2009). However, it is noteworthy that the surfactants used in this process are difficult to remove, resulting in toxicity in the organ. To solve these problems, several biocompatible polymers have been investigated for use as a base material to prepare CaP drug delivery and gene delivery systems in which the drugs or genes are adsorbed onto the surface of porous CaP (Cun et al., 2008; Schiffelers et al., 2005; Wang et al., 2010b).

In this study, we utilized biocompatible polymers (phosphatidylserine (PS)-poly(ethylene glycol) methyl ether (mPEG)) to assist in the preparation of CaP. Amphiphilic polymer PS-PEGs can self-assemble into micelles, and micelles can be used to carry non-polar drugs. The film dispersion method enables the hydrophobic side (PS) to easily pack inside the micelles and the hydrophilic side (PEG) to stay outside. PEGs enable the nanoparticles to escape from the phagocytosis of reticular endothelial cells, thereby increasing their time in the circulation and enhancing their accumulation in tumors. Because this polymer assists in the growth of CaP, PS-PEG/CaP hybrid porous nanospheres (PS-PEG/CaP nanospheres) can be prepared using a facile room-temperature approach. Porous CaP nanospheres can be used to adsorb drugs that differ from the drug inside the micelles. We then studied the morphology of the PS-PEG/CaP nanospheres and investigated their biocompatibility, and the main aim was to evaluate the potential application of PS-PEG/CaP nanospheres in drug delivery.

Methods

Materials

mPEG (Mn = 2000) was purchased from Sigma-Aldrich Co., Ltd. (Shanghai, China). Dulbecco's Modified Eagle's Medium (DMEM) was purchased from Hyclone (Logan, UT). N-(3-dimethylaminopropyl)-N′-ethylcarbodiimide hydrochloride (EDC) was purchased from Acros Organics Company (Geel, Belgium). Fetal bovine serum (FBS) was purchased from Gibco BRL (Australia). PS was purchased from Shanghai Yiji Medicine & Chemical Co., Ltd. (Shanghai, China). All chemical reagents were of analytical grade. Zebrafish and LO_2 cells (human normal liver cells) were purchased from the Institute of Biochemistry and

*These authors contributed equally to this work.

Correspondence: Yourong Duan. Tel/Fax: +86-21-64437139. E-mail: yrduan@shsmu.edu.cn
Zhirong Zhang. Tel: +86-28-85501566. Fax: +86-28-85501615. E-mail: zrzzl@vip.sina.com

Cell Biology, Chinese Academy of Sciences (Shanghai, China). The tumor necrosis factor (TNF)-α and interleukin (IL)-1β enzyme-linked immunosorbent assay (ELISA) test kits were purchased from the Beyotime Institute of Biotechnology (Shanghai, China).

Synthesis of mPEG–COOH

Pyridine (1.5 mL, 4 equiv.) and succinic anhydride (2 g, 4 equiv.) were added to a solution of mPEG (Mn = 2000; 10 g, 5 mmol, 1 equiv.) (mPEG) in 100 mL of dry $CHCl_3$. The reaction was stirred at 60 °C for 48 h with refluxing. The solvent was then removed under vacuum, and the residual solid was dissolved in 50 mL of saturated sodium hydrogen carbonate. The solution was extracted with $CHCl_3$ and washed with $MgSO_4$ to remove any trace water. The $CHCl_3$ solution was recrystallized from ether to obtain 8.6 g of a white powder (Chen et al., 2004; Corbin et al., 2007; Kim et al., 2005; Sun et al., 2012).

Synthesis of PS-mPEG

EDC (0.22 g) was added to a solution of mPEG–COOH (2.33 g) and PS (0.61 g) in 10 mL of dry $CHCl_3$. The solution was stirred at room temperature for 24 h and then concentrated and precipitated with ether. The precipitate was washed twice with ether and then dried under vacuum and stored at 4 °C (Kim et al., 2005; Sun et al., 2012). A schematic depicting the synthesis of PS-mPEG (PS-PEG) is shown in Figure 1.

Preparation of PS-mPEG/CaP hybrid porous nanospheres

PS-mPEG/CaP hybrid porous nanospheres (PS-PEG/CaP nanospheres) were prepared using the biomineralization method. Briefly, PS-PEG (20 mg) was dissolved in 5 mL of $CHCl_3$. The PS-PEG film was formed using rotary evaporation. Next, 50 mL of $CaCl_2$ (66.26 mg) was added to hydrate the film, and the pH was adjusted to 10 using 0.1 M ammonia followed by the addition of 50 mL of $(NH_4)_2$ HPO_4 (52.8 mg) dropwise into the solution. The mixture was stirred for 120 min at room temperature, and the pH was maintained at 9.5 *via* the addition of 0.1 M ammonia. The white precipitate was collected and washed by centrifugation–redispersion cycles twice with ethanol and twice with deionized water and then dried under vacuum at 37 °C (Chen et al., 2011, 2012; Ginebra et al., 2012; Qi et al., 2012). A schematic depicting the synthesis of the PS-mPEG (PS-PEG) is shown in Figure 2. CaP nanospheres were prepared under similar conditions.

Characterization of PS-PEG/CaP nanospheres

The size and size distribution of the PS-PEG/CaP nanospheres were evaluated using the Zetasizer IV (Malvern Zetasizer Nano ZS90, Malvern, Worcestershire, UK). TEM (H-800; Hitachi, Tokyo, Japan) was used to observe the morphology of the PS-PEG/CaP nanospheres. ^{1}H NMR spectra were recorded on a Bruker Avance 400 NMR spectrometer (Bruker Avance, Switzerland). X-ray diffractometry was performed on the

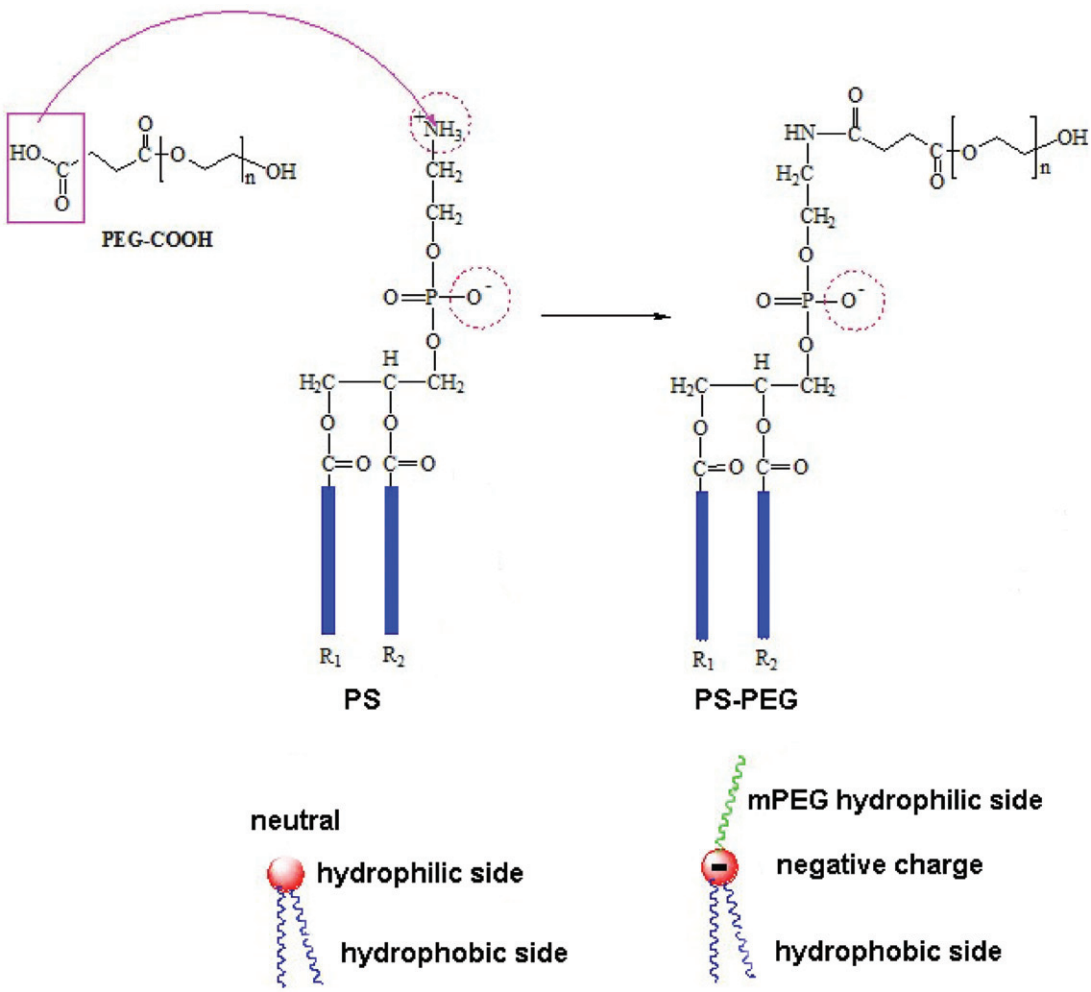

Figure 1. Synthesis schematic for PS-mPEG. PS are non-charged amphiphilic molecules with a small polar head and two long nonpolar tails. mPEGs are hydrophilic macromolecules. mPEGs were used to modify the polar head of the PS to form negatively charged amphiphilic macromolecules.

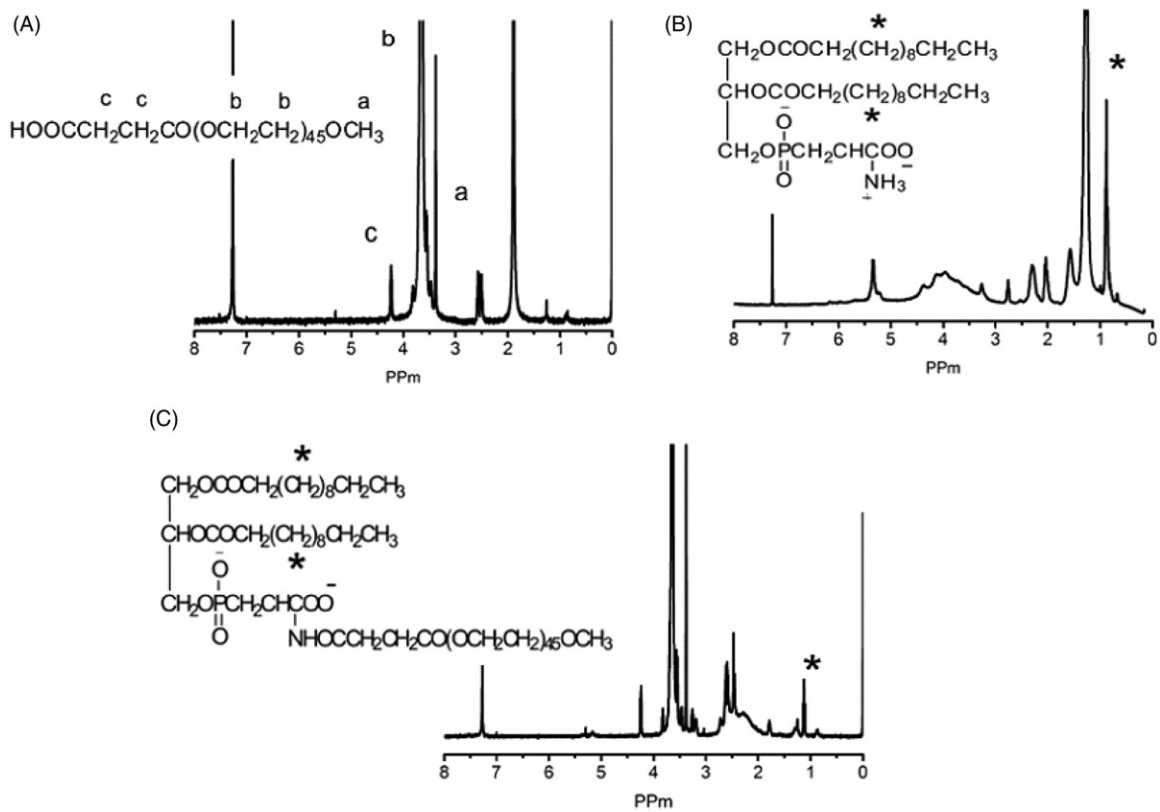

Figure 2. ^{1}H NMR spectra of PEG–COOH (A), PS (B) and PS-PEG (C).

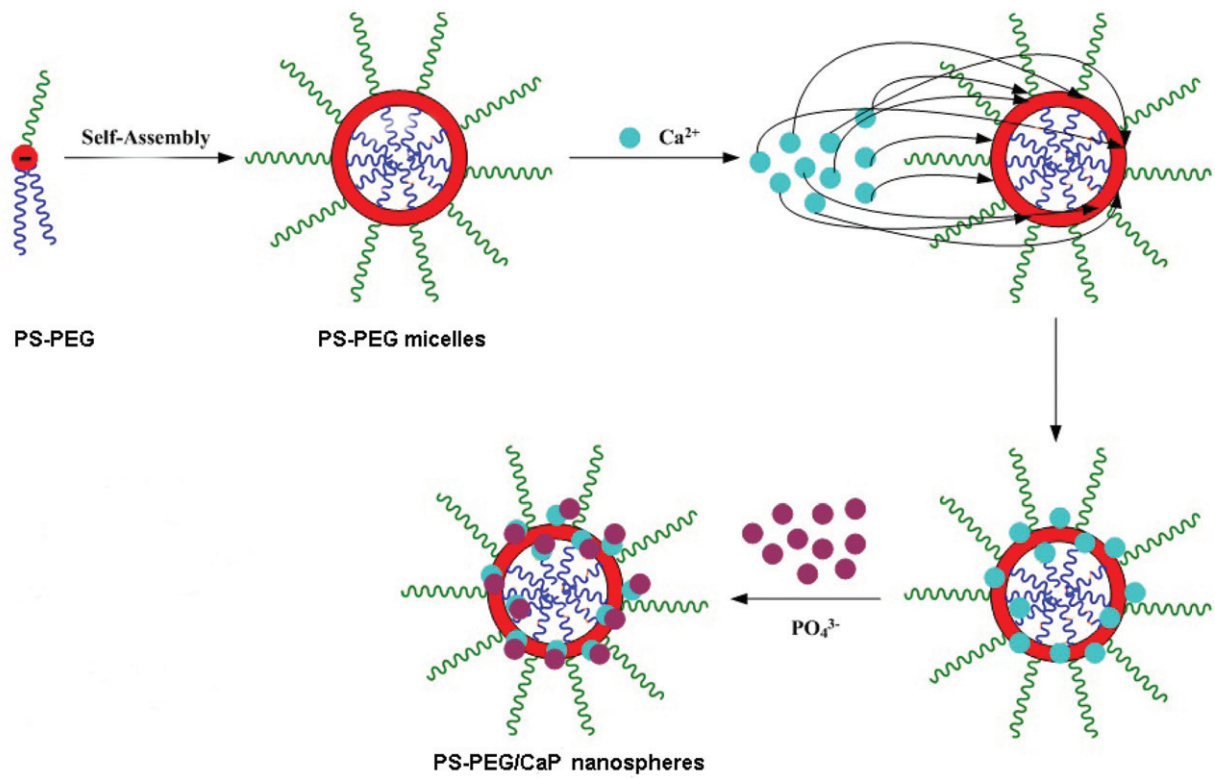

Figure 3. Preparation of PS-PEG/CaP nanospheres. Negatively charged amphiphilic PS-PEG macromolecules form micelles via self-assembly and are nonpolar inside and amphiphilic outside. Negatively charged micelles can adsorb positively charged Ca^{2+}, and PO_4^{3-} is subsequently attached to the micelles to form CaP nanospheres.

PS-PEG, CaP nanospheres and PS-PEG/CaP nanospheres using a Phillips X'pert PORMPO diffractometer. A Cu Kα radiation source was used, and the scanning rate was 5 °C/min. TGA (TA, TGA2050) was performed to characterize the thermal stability of the PS-PEG, CaP nanospheres and PS-PEG/CaP nanospheres. TGA measurements were performed with a heating rate of 10 °C min^{-1} in air (Wang et al., 2011).

Hemocompatibility evaluation

Hemolysis

Fresh blood obtained from a healthy rabbit containing sodium citrate (3.8 wt%) in a ratio of 9:1 was diluted in saline (8 mL of fresh rabbit blood was diluted with the addition of 10 mL saline). PS-PEG and PS-PEG/CaP nanospheres were suspended in 10 mL of 0.9% NaCl solution. PS-PEG and PS-PEG/CaP nanospheres (5 mg/mL) solution were incubated for 1 h at 37 °C in a shaking water bath. Diluted blood (0.2 mL) was added to the suspensions and incubated for 1 h. Positive and negative controls were generated by adding 0.2 mL of diluted blood to 10 mL of distilled water or saline, respectively. Hemoglobin release was determined after centrifugation (3000 rpm for 5 min), and a photometric analysis of the supernatant was performed at 545 nm. The hemolytic ratio (HR) was calculated from the optical density (OD) data of the test sample, positive control and negative control using the equation below, and all of the data were calculated based on the average of three replicates (Andrade et al., 2011; Sangeetha et al., 2013; Wang et al., 2008).

$$\mathrm{HR}(\%) = \frac{100(\mathrm{OD}_{\text{test sample}} - \mathrm{OD}_{\text{negative control}})}{(\mathrm{OD}_{\text{positive control}} - \mathrm{OD}_{\text{negative control}})}$$

Plasma recalcification profiles

Platelet-poor plasma (PPP) was prepared by centrifuging whole blood (containing 3.8 wt% citrate acid solution, blood/citrate acid = 9:1), which was isolated from a healthy rabbit, at 3000 rpm for 10 min. PS-PEG and PS-PEG/CaP nanospheres samples were prepared by dissolving the samples in 0.025 M $CaCl_2$ to a concentration of 5 mg/mL. Next, 100 μL of the sample was added into a siliconized glass tube.

A volume of 100 μL of PPP was preheated to 37 °C and added to the samples. After 50–200 s, the tube was tilted every 1–2 s to observe the clotting time. The glass tube was used as a positive control, and the siliconized glass tube was used as a negative control (Nie et al., 2007).

Quantification of blood clotting time

PS-PEG and PS-PEG/CaP nanospheres were dissolved in $CaCl_2$ solution (0.2 mol L^{-1}) to obtain a concentration of 5 mg/mL. Next, 0.025 mL of the sample was added into a siliconized glass tube. The glass tube served as the positive control, and the siliconized glass tube served as the negative control.

The test tubes were placed in a thermostat at 37 °C for 5 min. ACD whole blood (0.2 mL) (containing 3.8 wt% citrate acid solution, blood/citrate acid = 9:1) was subsequently added to the tubes. At specific time points, 50 mL of distilled water was gently added to the tubes. The OD of the supernatant was determined at a wavelength of 545 nm using a spectrophotometer. The relative absorbency of 0.2 mL ACD whole blood diluted in 50 mL distilled water was assumed to be 100. The blood clotting index (BCI) of the biomaterials was quantified using the ratio of the absorbency of the blood that was in contact with the sample compared to the solution of distilled water and ACD blood. The relative clotting time of each sample was obtained from the OD versus time plots.

Cytocompatibility evaluation

MTT assay

The liver is the most important detoxification organ, rapidly receiving all of the drugs injected into the veins. Because they are a site of collection of intravenous drugs, it is necessary to evaluate the toxicity of these drugs for liver cells. LO_2 cells (normal human liver cell line) were cultured in DMEM (Gibco) with 10% FBS (Gibco), 100 U/mL penicillin and 100 μg/mL streptomycin in a humidified atmosphere of 5% CO_2 at 37 °C. Stock solutions were prepared by dissolving the PS-PEG and PS-PEG/CaP nanospheres in culture medium. A series of dilutions were obtained from the stock solutions with the addition of medium to obtain final concentrations of 1, 10, 50, 200 and 1000 μg/mL. DMEM culture medium was used as a negative control. The cells were then incubated in 96-well cell culture plates at 1×10^3 cells/100 μL medium in each well for 24 h. The medium was then replaced with 100 μL samples. After incubating for 24, 48 and 72 h, the medium was removed and replaced with 20 μL of MTT solution at the end of each incubation time and then incubated for an additional 4 h. Next, the medium was removed and replaced with 150 μL of DMSO. After gentle shaking for 10 min, the OD was determined using an ELISA reader at a wavelength of 545 nm. All of the experiments were performed in triplicate. The cell viability was calculated from the OD value of the test sample and a negative control using the equation below, and the data were represented as the mean ± SD.

$$\text{Relative activity}(\%) = 100 \times \frac{\mathrm{OD}_{\text{test sample}}}{\mathrm{OD}_{\text{negative control}}}$$

Analysis of cellular toxicity

Cellular toxicity was determined by measuring the LDH release from LO_2 cells using the CytoTox 96® non-radioactive cytotoxicity assay (Promega Medical Supply Company Ltd., Dublin, Ireland). A 6.4% phenol solution diluted in medium was used as a positive control, and culture medium was used as a negative control. Following 24 h of incubation in 96-well dishes, the LO_2 cells were exposed to 100 μL of PS-PEG and PS-PEG/CaP nanospheres solutions (5 mg/mL), respectively. At 24-h post-incubation, the culture medium was collected and centrifuged at 1500 rpm for 10 min. The lactate dehydrogenase activity was then assayed in the supernatant by measuring the changes of absorption at 340 nm due to the oxidation of NADH (Han et al., 2005; McGinley et al., 2011; Muzzarelli et al., 2005).

Analysis of inflammatory cytokine release

THP-1 cells, a human monocytic leukemia cell line obtained from the Institute of Biochemistry and Cell Biology, Chinese Academy of Sciences (Shanghai, China), were cultured in RPMI supplemented with 10% FBS, 2 mM glutamine, 1.5 mg/mL glucose, 100 UI cm^{-3} penicillin and 100 μg/mL of streptomycin. The cells were seeded into 96-well, flat-bottom plates (Nunc, Penfield, NY) after stimulation with phorbol 12-myristate 13-acetate (PMA). This chemical induces the differentiation of cells into adherent macrophages, thus terminating their natural proliferation. THP-1 cells and 25 ng mL^{-1} PMA in RPMI media were added at 200 μL/well into wells using a Matrix WellMate (Thermo Fisher Scientific, Waltham, MA). The plates were incubated for 72 h in the above conditions to enable the THP-1 cells to adhere to the bottom of the wells.

The growth medium was separately replaced with PS-PEG and PS-PEG/CaP nanospheres solutions (5 mg/mL). A 6.4% phenol solution in medium was used as a positive control. After 24 h, the culture medium was collected for measurement. All of the experiments were performed in triplicate. The concentrations of TNF-α and IL-1β were determined using ELISA (Malafaya et al., 2007; Morishige et al., 2010; Salah et al., 2013).

Long-term effects after a single loading of PS-PEG/CaP nanospheres into zebrafish

Biodistribution in the larvae after the loading of FITC-PS-PEG/CaP nanospheres into the bloodstream

An FITC solution in DMSO (1 mg/mL) was mixed with an aqueous solution of PS-PEG (pH = 9). The reaction was performed in the dark at 4 °C for 12 h. The reaction mixture was dialyzed in deionized water for three days to obtain the FITC-labeled PS-PEG sample (FITC-PS-PEG). Next, FITC-PS-PEG was used to prepare the FITC-PS-PEG/CaP nanospheres.

Microangiography was used to introduce the FITC-PS-PEG/CaP nanospheres into the circulatory system of zebrafish embryos. Selected zebrafish embryos at 72 hpf were mounted laterally in 0.3% agarose and covered with embryo culture medium. The FITC-PS-PEG/CaP nanospheres were then injected into the sinus venosus. After the injection, the FITC-PS-PEG/CaP nanospheres circulated throughout the entire vascular network, where each blood vessel could be visualized using a fluorescent microscope. Embryos loaded with FITC-PS-PEG/CaP nanospheres in the blood system were examined at 4 h, 24 h, 48 h and 72 h post-microinjection on a Zeiss LSM410 system (LSM 410, Zeiss, Jena, Germany), and confocal images were obtained for further analysis (Bekyarova et al., 2005).

Acridine orange staining

Cell apoptosis in the embryos was identified using acridine orange (AO) staining. AO is a nucleic acid-selective metachromatic stain used to study apoptosis patterns. After 24 h, 48 h, 72 h and 96 h of exposure to the PS-PEG/CaP nanospheres (5 mg/mL), 10 larvae from each beaker ($n = 3$) were washed twice in 30% Danieau's solution (58 mM of NaCl, 0.7 mM of KCl, 0.4 mM of $MgSO_4$, 0.6 mM of Ca $(NO_3)_2$ and 5 mM of HEPES, pH 7.4) and transferred into 5 µg/mL of AO dissolved in 30% Danieau's solution for 20 min at room temperature. The larvae were then washed with 30% Danieau's solution three times for 5 min. The apoptotic cells were identified using a fluorescence microscope (Nikon, Tokyo, Japan) (Deng et al., 2009).

Results and discussion

Synthesis of PS-mPEG

A schematic depicting the synthesis of PS-mPEG is shown in Figure 1. PS are amphiphilic molecules, which are widely used to

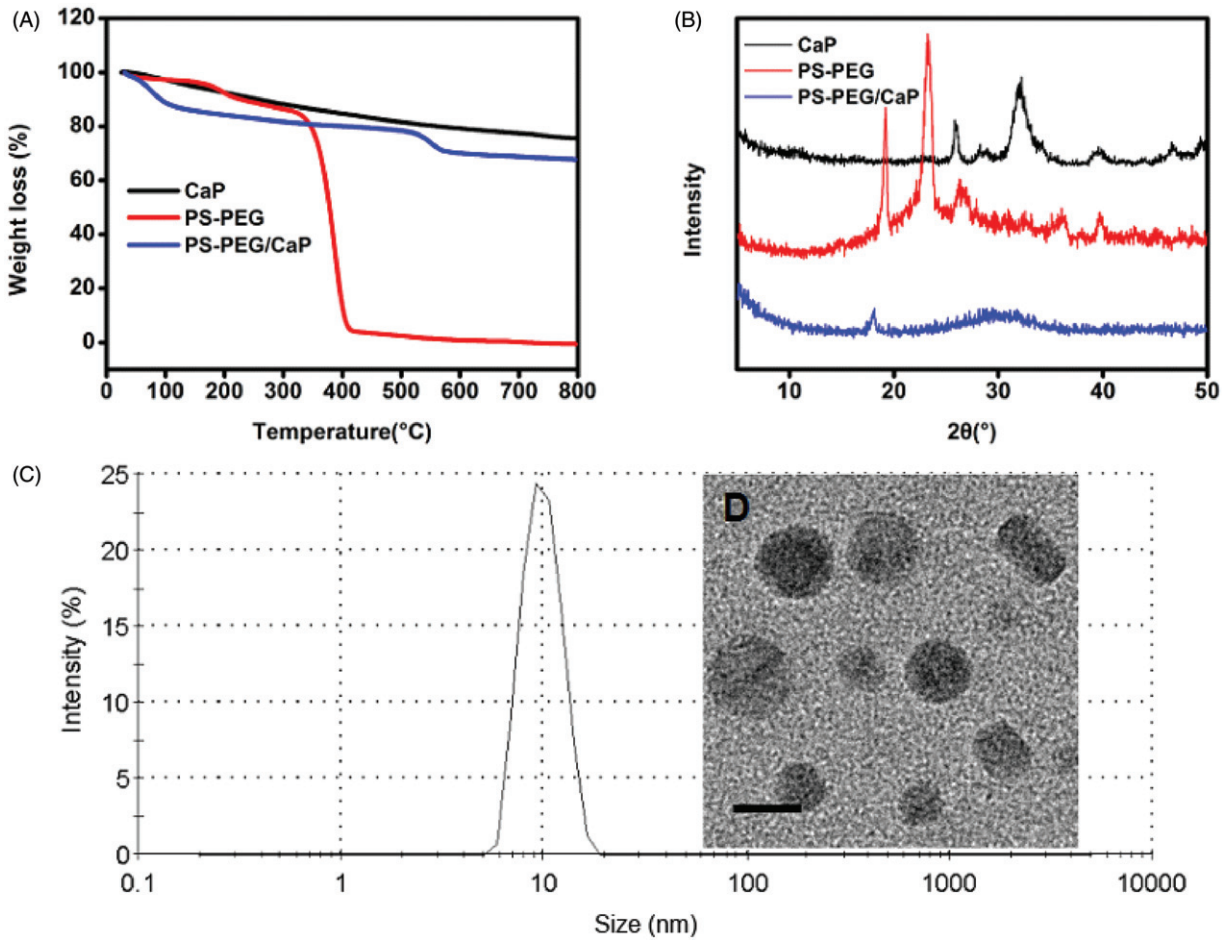

Figure 4. Characterization of PS-PEG/CaP nanospheres. TGA curves for CaP nanospheres, PS-PEG and PS-PEG/CaP nanospheres (A). PS-PEG/CaP exhibited a prolonged weight drop in temperature for PS-PEG; X-ray diffraction of CaP nanospheres, PS-PEG and PS-PEG/CaP nanospheres (B). PS-PEG and CaP presented a crystalline structure, where only a small peak of PS-PEG could be found in the PS-PEG/CaP nanospheres. No CaP peaks were found in the PS-PEG/CaP nanospheres; size distribution of the PS-PEG/CaP nanospheres (C). The size peak of the PS-PEG/CaP nanospheres was 10 nm; TEM images of the PS-PEG/CaP nanospheres (D). The PS-PEG/CaP nanospheres were spherical. Bar is 10 nm.

prepare various pharmaceutical formulations. As the most important component of the cell membrane, PS are non-toxic to the body and are feasible to cell uptake. Because the polar head and nonpolar tails of PS are asymmetrical, a polarity chain is introduced to modify the PS. mPEGs are hydrophilic macromolecules that can be used to modify the polar heads of the PS to form amphiphilic macromolecules. First, the hydroxyl group of mPEG reacted with succinic anhydride to form mPEG–COOH. Subsequently, the carboxyl group was modified with EDC, and the mixture of the mPEG–COOH with PS was stirred at room temperature to form PS-mPEG. The ^{1}H NMR spectra of PEG–COOH (A), PS (B) and PS-PEG (C) are shown in Figure 3. Proton signals of the PEG–COOH molecules (a: $-OCH_3$ at d 3.38, b: $-OCH_2CH_2-$ at d 3.64 and c: $-OCCH_2CH_2CO-$ at d 4.23) could be observed in the PS-PEG molecules. The peak present at d 1.12 was $-CH_2-$ from the PS molecules.

A schematic of the preparation method used to generate PS-PEG/CaP nanospheres is depicted in Figure 2. Amphiphilic PS-PEG macromolecules can easily form micelles *via* self-assembly. The film dispersion method was used to prepare micelles with a hydrophobic chain inside and a hydrophilic chain (PEG side) outside. This structure enables the micelles to carry hydrophobic drugs. Negative PS-mPEGs are conductive for Ca^{2+} adsorption and form a CaP shell. PS-PEG-assisted CaP nanospheres are formed by the addition of $CaCl_2$ and $(NH_4)_2HPO_4$ in a dropwise manner. The porous CaP can absorb both hydrophobic and hydrophilic drugs. Thus, PS-PEG/CaP nanospheres can be used to carry two different types of drugs for different purposes. In addition, the PEG chain contributes to increase long residence time of the drug carrier in the blood.

Characterization of PS-PEG/CaP nanospheres

PS-PEG/CaP nanospheres were prepared using a facile room-temperature approach. The natural composition of the particles can be elucidated *via* their oxidative thermal weight-loss response. A composition of approximately 90% CaP and 10% organics was found using TGA as shown in Figure 4(A). CaP nanospheres exhibited a negligible weight loss. However, PS-PEGs exhibited a decomposition pattern of increased weight loss. The decrease in weight was caused by the decomposition of the polymer segments at 300–400 °C. The weight loss temperature (500 °C–600 °C) of PS-PEG/CaP nanospheres was higher than that of PS-PEG, indicating that PS-PEG was protected by the CaP shell.

X-ray diffraction is an effective method for investigating polymorphic modifications. X-ray diffractograms of the PS-PEG, CaP nanospheres and PS-PEG/CaP nanospheres are shown in Figure 4(B). CaP nanospheres exhibit a number of sharp crystalline peaks ($2\theta = 25.8$, $d = 97$ Å; $2\theta = 32.2$ $d = 183$ Å) and PS-PEG also exhibit a number of sharp crystalline peaks ($2\theta = 19.2$, $d = 322$ Å; $2\theta = 23.3$ $d = 455$Å). In contrast, PS-PEG/CaP nanospheres present a weak peak at $2\theta = 18.5$, $d = 322$ Å. These results not only confirmed that the PS-PEG was incorporated into the CaP shells but they also demonstrated that the CaP shell of the PS-PEG/CaP nanospheres were more amorphous compared to the CaP nanospheres. A less-ordered crystal lattice is known to favor drug inclusion. Thus, the amorphous shape of the PS-PEG/CaP nanospheres is conducive to drug loading.

The size and size distribution of the PS-PEG/CaP nanospheres were evaluated using a Zetasizer (Figure 4C). The PS-PEG/CaP nanospheres exhibited a particle size of 9.93 ± 2.13 nm and a polydispersity index of 0.149 ± 0.002. TEM images of the PS-PEG/CaP blank nanospheres are shown in Figure 4(D). The porous nanospheres with 10 nm diameter have many nanometer-sized pores, which are conducive to a high drug-loading capacity. Nanospheres with a small size can accumulate in tumor tissue, suggesting that PS-PEG/CaP nanospheres may also be suitable to carry cancer drugs.

Hemocompatibility evaluation

Hemolysis

A hemolytic rate experiment was used to evaluate the degree of hemolysis and free hemoglobin of biomedical materials *in vitro*. A higher hemolytic rate indicates a higher degree of destruction of red blood cells. A high plasma hemoglobin level normally indicates hemolysis and reflects erythrocyte membrane fragility in contact with materials. The color of the positive tubes appeared dark red (indicating ruptured erythrocytes), whereas the negative tubes were transparent and the erythrocytes remained at the bottom of the tubes (Figure 5A). Similar phenomena were observed in PS-PEG and PS-PEG/CaP nanospheres tubes. The HR of PS-PEG and PS-PEG/CaP were 4.21% and 0.76%, respectively, as listed in Table 1, the OD values of both negative and positive controls were within the recommended range according to the ISO 10993-4. Both the image in Figure 5(A) and data in Table 2 confirmed that PS-PEG and PS-PEG/CaP did not induce hemolysis.

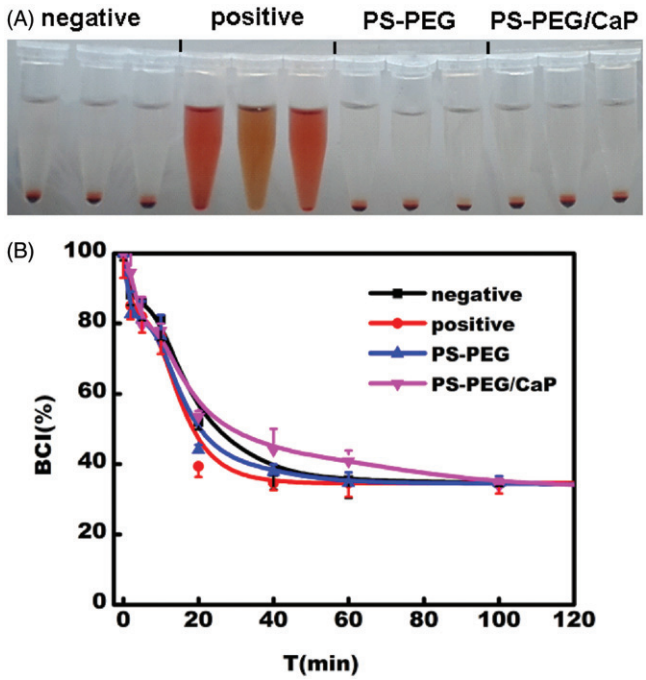

Figure 5. Hemolytic images (A). Red blood cells that did not hemolyze fell to the bottom of the tubes in the negative control, PS-PEG and PS-PEG/CaP nanospheres groups. The color of the hemolyzed positive control was red. Dynamic blood clotting profiles of PS-PEG and PS-PEG/CaP nanospheres (B). At 40 min, the BCI of the positive control did not change, and the negative controls and PS-PEG were unchanged at 70 min, which was similar to the PS-PEG/CaP nanospheres at 100 min. Data were represented as mean ± SD ($n = 3$).

Table 1. Hemolytic activity.

Sample	OD at 545 nm	Hemolysis ratio (%)
Distilled water	0.850 ± 0.021	+ve control
Saline	0.032 ± 0.009	−ve control
PS-PEG	0.066 ± 0.011	0.0421
PS-PEG/CaP	0.038 ± 0.008	0.0076

Data are represented as mean ± SD ($n = 3$).

Measurement of plasma recalcification profiles

The effect of the materials on clotting time was evaluated using the plasma recalcification time (PRT) test. The PRT of a material is significant if the material is able to prolong by 40% the silicification of glossy glass.

As shown in Table 2, the PRT of the PS-PEG and PS-PEG/CaP nanospheres was similar to that of the negative control but longer compared to the positive control. Moreover, the PRT for each test material was 40% longer than the positive control, indicating that both PS-PEG and PS-PEG/CaP nanospheres did not exhibit an obvious effect on the intrinsic coagulation pathway.

Quantification of whole blood clotting time

Coagulation is a process in which blood is transformed from the flow state to the gel state, and this process is referred to as a change from soluble plasma fibrinogen into insoluble fibrin. In this study, the dynamic blood clotting profiles of PS-PEG and PS-PEG/CaP nanospheres were evaluated. Dynamic clotting time tests were performed to observe the effect of the materials on clotting time when the samples were in contact with blood. As shown in Figure 5(B), the slower the decrease in BCI with time, the longer the clotting time. All of the samples and controls demonstrated a rapid decrease in the BCI. The positive control showed the most rapid decrease in BCI, with a whole clotting time of 40 min. The whole clotting time of the PS-PEG and negative control were similar, i.e. 70 min, whereas that of the PS-PEG/CaP was 100 min, indicating that PS-PEG and PS-PEG/CaP nanospheres did not interact with the fibrinogen in the blood.

Table 2. Data of plasma recalcification time of materials.

Sample	Time
Negative	163 ± 5
Positive	110 ± 5
PS-PEG	165 ± 8
PS-PEG/CaP	167 ± 7

Data are represented as mean ± SD ($n = 3$).

Cytocompatibility evaluation of PS-PEG/CaP nanospheres

MTT assay

The cellular toxicity of the materials was evaluated using the MTT assay. LO_2 cells were selected to evaluate the toxicity of the materials for biocompatibility evaluation. If nanospheres are injected, then the liver is an important organ that comes into contact with the nanospheres after entering the blood circulation. In this study, we selected the LO_2 cell line to evaluate cellular toxicity.

The cell viability of LO_2 cells cultured with PS-PEG and PS-PEG/CaP for 24 h (A), 48 h (B) and 72 h (C) are shown in Figure 6. The viability of the LO_2 cells slightly varied with the incubation time as well as the concentration of PS-PEG and PS-PEG/CaP nanospheres. Even at the longest time and at the highest concentration (the highest concentration that can be used in the drug-delivery experiment), the relative activity (%) was higher than 80% for both PS-PEG and PS-PEG/CaP nanospheres. According to the United States Pharmacopoeia standards, this finding indicated that these materials were not toxic to LO_2 cells.

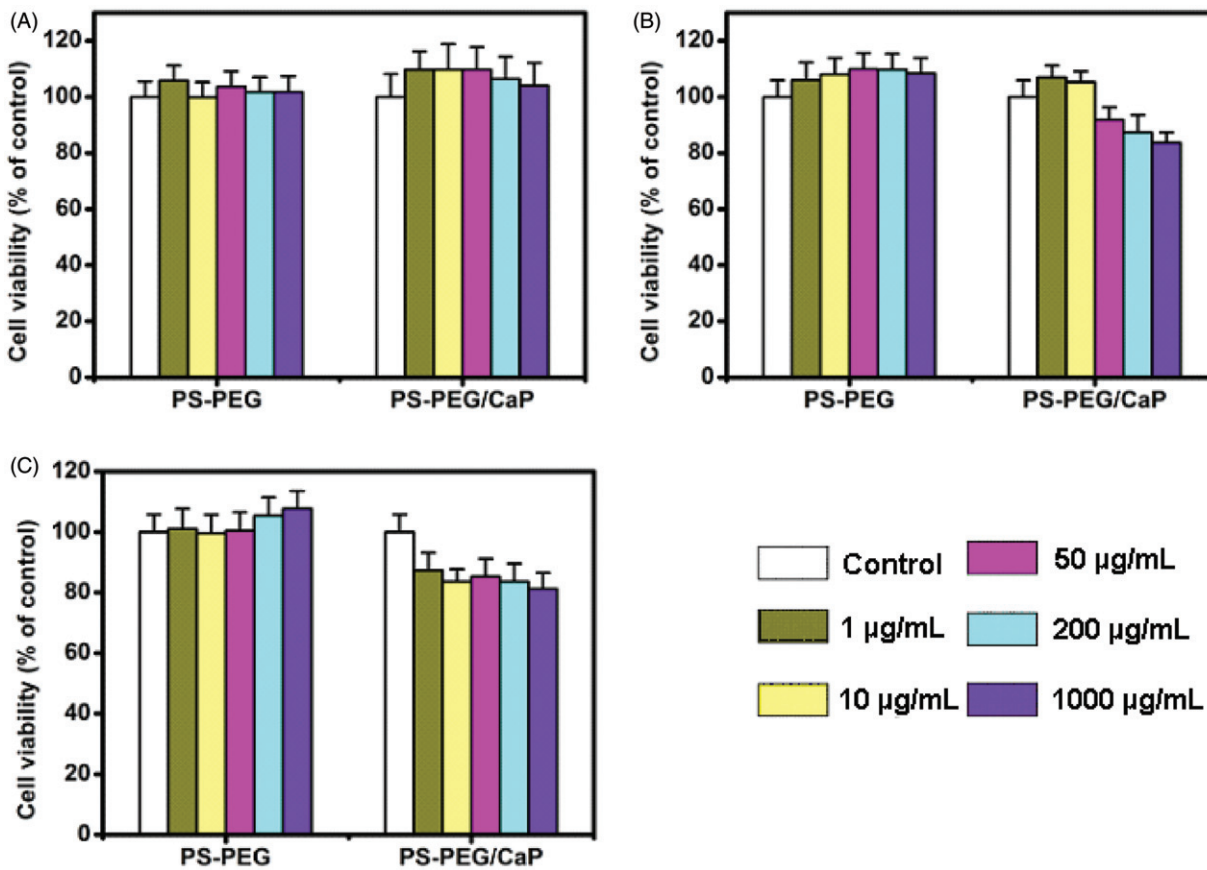

Figure 6. LO_2 cell viability after culture in the PS-PEG and PS-PEG/CaP solutions for 24 h (A), 48 h (B) and 72 h (C). The cell viability was not affected after treatment with PS-PEG for 24 h, 48 h and 72 h. Time had little effect on cell viability in the PS-PEG/CaP group. Cell viability was slightly decreased with an increase in the concentration of PS-PEG/CaP. Data were represented as mean ± SD ($n = 3$).

Analysis of cellular toxicity by LDH

LDH is a stable cytoplasmic enzyme present in all living cells. LDH activity detects the integrity of the cell membrane and reflects the state of mitochondrial metabolism and function.

LDH release from LO_2 cells exposed to the samples was evaluated as an indicator of cellular toxicity. The release of LDH enzyme from the LO_2 cells at 24 h in the sample solutions is listed in Table 3. The LDH concentration released from the cells in the negative control group was 16.91 pg/mL, whereas the LDH concentration in the positive control (6.4% phenol) group was 47.03 pg/mL. The LDH concentration in PS-PEG and PS-PEG/CaP nanospheres groups was 21.82 pg/mL and 9.84 pg/mL, respectively, suggesting that the LDH release was lower for PS-PEG/CaP nanospheres compared to PS-PEG and much lower compared to the positive control. These results were consistent with the results obtained from the MTT tests, indicating that the polymers exhibited negligible toxicity.

Table 3. Extracellular content of LDH in L929 cell line.

Sample	Concentartion of LDH (pg/mL)
Positive	470.3 ± 4.11
Negative	16.91 ± 5.97
PS-PEG	21.82 ± 6.70
PS-PEG/CaP	9.84 ± 4.32

Data are represented as mean ± SD ($n = 3$).

Analysis of inflammatory cytokine release using ELISA

The pro-inflammatory cytokine IL-1β is involved in the initiation of inflammatory processes and contributes to inflammatory diseases. In addition, TNF-α promotes leukocyte activation and enhances the release of an array of inflammatory factors and destructive enzymes. Thus, we performed systematic studies to determine the association between IL-1β and TNF-α.

TNF-α and IL-1β levels in the culture medium of the samples were measured using ELISA. As a positive control, 6.4% phenol treatment was used to induce the production of inflammatory cytokines. The extracellular content of TNF-α and IL-1β in the THP-1 cell line after 24 h of culture is shown in Figure 7(D) and (E). The amount of TNF-α release was 7.2 and 8.4 pg/mL for PS-PEG and PS-PEG/CaP nanospheres, respectively, which was lower than that of the positive control (10.4 pg/mL). For IL-1β, the release of IL-1β was 9.2 and 8.7 pg/mL for PS-PEG and PS-PEG/CaP nanospheres, respectively, which was much lower than that of the positive control (12.6 pg/mL). Thus, the effects of PS-PEG and PS-PEG/CaP nanospheres on cytokine production were significantly lower compared to the positive control, which might be attributed to an inhibitory effect of the extracts on

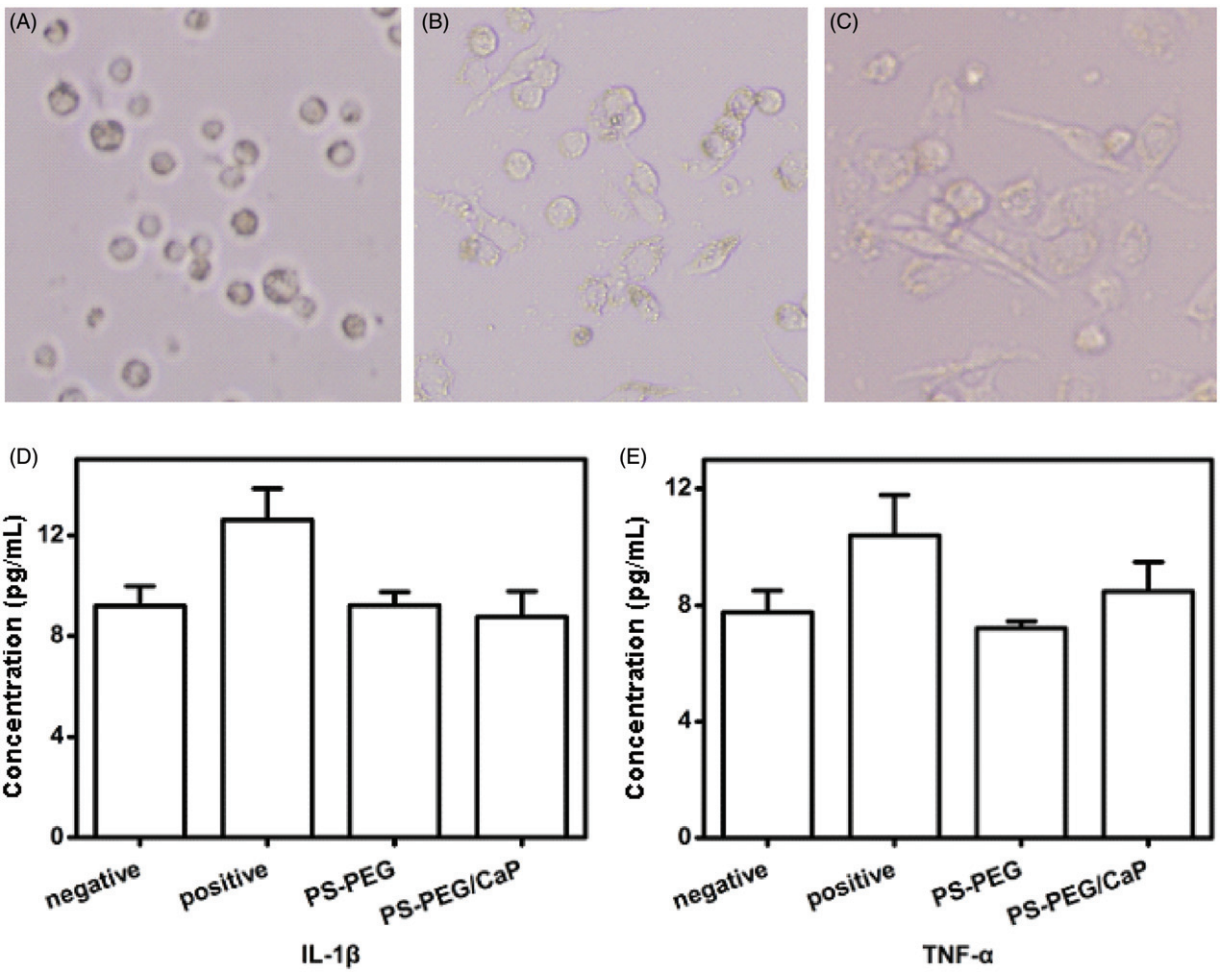

Figure 7. Phorbol 12-myristate 13-acetate (PMA) induced the differentiation of THP-1 cells into adherent macrophages: 0 h (A), 24 h (B), 48 h (C). At 0 h, the THP-1 cell was spherical and not adherent. After 24 h, the THP-1 cells began to adhere and some of the cells were beginning to deform. After 48 h, the cells had completely deformed and pseudopodia had formed. The extracellular contents of IL-1β (D) and TNF-α (E) in the THP-1 cell line after 24 h in culture. The IL-1β concentrations of the negative control, PS-PEG group and PS-PEG/CaP group were lower compared to the positive control. The TNF-α concentration of the PS-PEG/CaP group was higher compared to the negative control and PS-PEG group but lower than the positive control group. Data were represented as mean ± SD ($n = 3$).

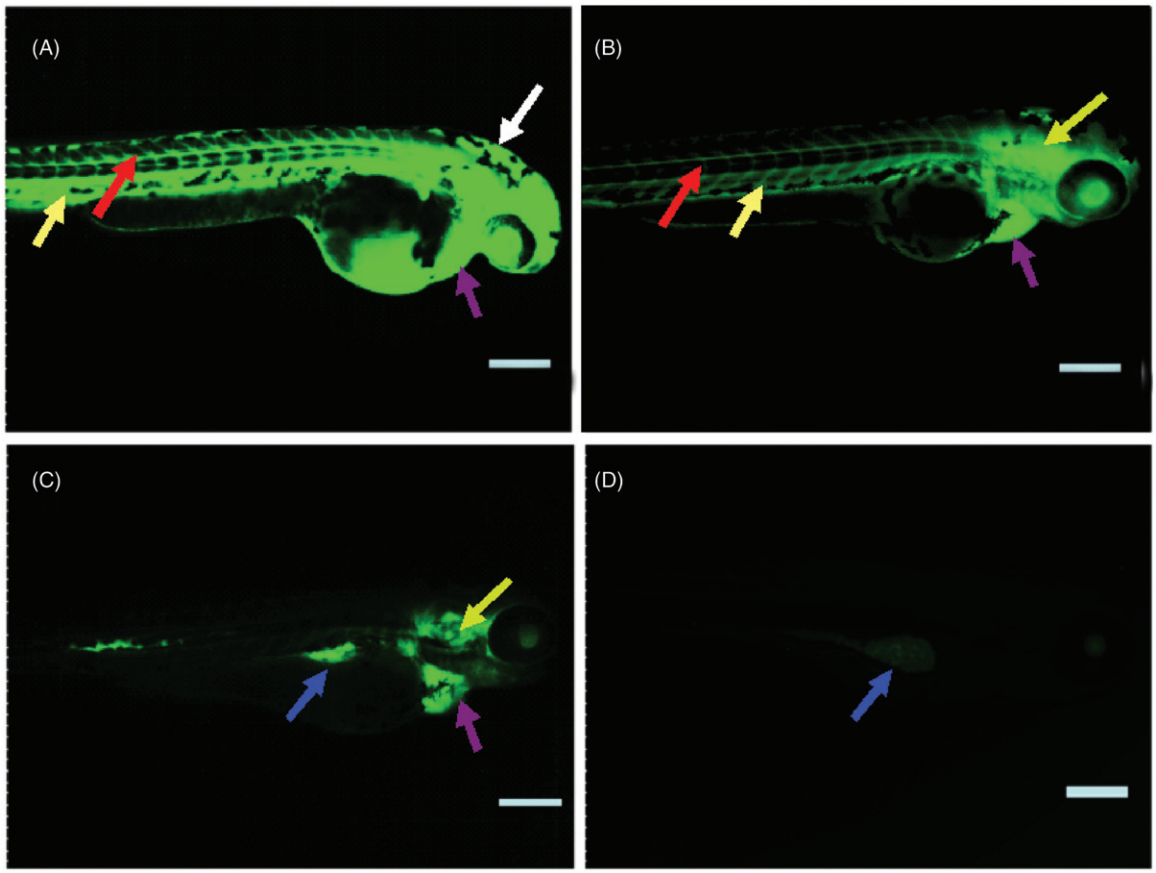

Figure 8. *In vivo* biodistribution and clearance of FITC-PS-PEG/CaP nanospheres in zebrafish larvae via intravascular loading at 72 hpf. The intravascular loaded FITC-PS-PEG/CaP nanospheres reached the floor plate (red arrow), ventricle (white arrow) and blood vessels (yellow arrow) within 4 h (A). Most of the loaded FITC-PS-PEG/CaP nanospheres gradually accumulated in the heart (purple arrow), blood vessels and digestive organs (green arrow) after 24 h. After 48 h following the delivery, nanospheres accumulated in the swim bladder region of the larvae (blue arrow). The intravascular-loaded FITC-PS-PEG/CaP nanospheres were gradually excreted from the embryos, and there was no detectable signal at approximately 72 h after delivery (D). Scale bar is 200 μm.

leukocyte activation, resulting in a reduction in the release of inflammatory mediators and pro-inflammatory cytokines as well as an amelioration of inflammation. These findings indicate that the PS-PEG/CaP nanospheres have excellent biocompatibility.

Biodistribution and clearance of FITC-PS-PEG/CaP nanospheres in zebrafish larvae when loaded into the cardiovascular system

The biodistribution and clearance of FITC-PS-PEG/CaP nanospheres in zebrafish larvae were examined by introducing FITC-PS-PEG/CaP nanospheres into the cardiovascular system at 72 hpf *via* intravascular loading. As shown in Figure 8, the FITC-PS-PEG/CaP nanospheres were first distributed throughout the blood circulatory system and then moved into the muscles and other tissues. The FITC-PS-PEG/CaP nanospheres migrated into the floor plate, brain ventricle, blood vessels and nearly all other organs in the larvae at 4 h after loading (Figure 8A). The loaded FITC-PS-PEG/CaP nanospheres accumulated in the heart, blood vessels and digestive organs after 24 h (Figure 8B). The injected FITC-PS-PEG/CaP nanospheres had a long circulatory residence time. The zebrafish larvae exhibited highly concentrated FITC-PS-PEG/CaP nanospheres in the heart and swim bladder, but no detectable fluorescent signal of the FITC-PS-PEG/CaP nanospheres was observed in the other organs after 48 h (Figure 8C). Because the swim bladder is known to be a detoxifying organ, these results indicated that the zebrafish larvae effectively filtered out the injected nanoparticles. These FITC-PS-PEG/CaP nanospheres were gradually excreted from the zebrafish larvae, and there was no detectable signal at approximately 72 h after delivery (Figure 8D).

AO staining

After exposure to PS-PEG/CaP for 24 h, 48 h, 72 h and 96 h, the larvae were stained with AO. As shown in Figure 9, no obvious apoptotic cells were observed in the control larvae or the nanospheres-treated group at all time periods, suggesting that the PS-PEG/CaP nanospheres did not induce apoptosis.

Conclusions

PS-mPEG was successfully synthesized by grafting PS to mPEG–COOH, and PS-PEG/CaP hybrid porous nanospheres were prepared using a facile polymer-assisted method at a relatively low temperature. The hybrid PS-PEG/CaP nanospheres with a porous structure had a diameter of 10 nm. X-ray diffractometry and TGA confirmed that PS-PEGs were incorporated into the CaP shells. PS-PEG/CaP nanospheres, which were present at a low HR, demonstrated negligible toxicity and served as an excellent anticoagulant. The results obtained from the zebrafish experiment confirmed that the PS-PEG/CaP nanospheres exhibited a long circulatory residence time *in vivo* and did not induce cellular apoptosis. Taken together, these findings suggest that PS-PEG/CaP nanospheres exhibit excellent biocompatibility and have potential use as drug-delivery carrier.

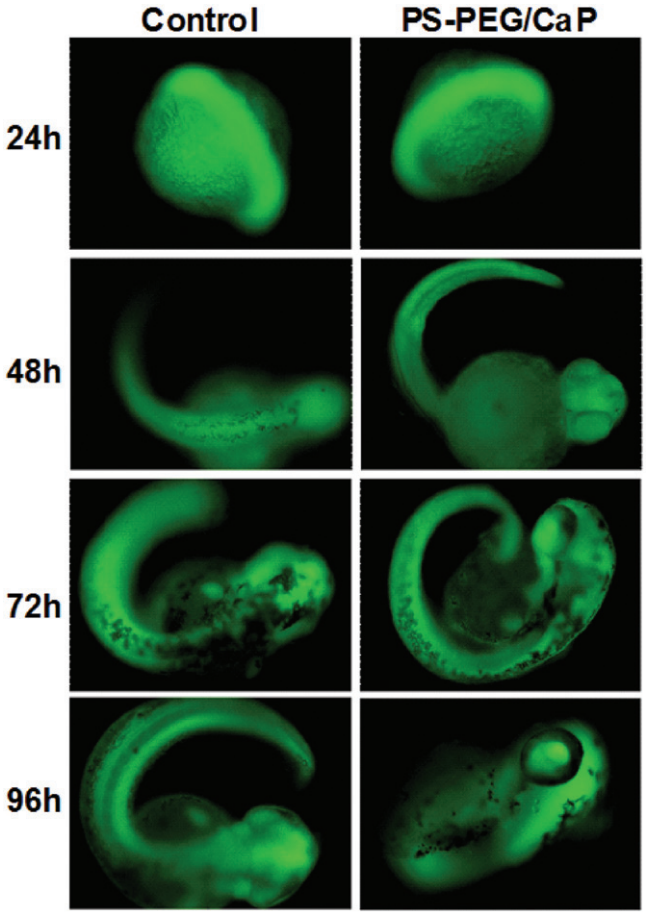

Figure 9. Zebrafish exposed to PS-PEG/CaP were stained with acridine orange (AO). No AO-positive apoptotic cells were found in the control and PS-PEG/CaP groups. (A) 24 h, (B) 48 h, (C) 72 h and (D) 96 h.

Declaration of interest

The authors report no conflicts of interest. The authors alone are responsible for the content and writing of this article.

This work was supported by the 973 Program of the Chinese Government (No. 2009C930300), National Science Foundation of People's Republic of China (Nos. 30430770, 81272568 and 81101738), the International Cooperation Project from the Science and Technology Commission of Shanghai (No. 13430722200), the Scientific Research Innovation Program from the Shanghai Municipal Education Commission (14YZ029) and the program for National S & T Major project of China (2011ZX09501-001-01).

References

Andrade FK, Silva JP, Carvalho M, Castanheira EMS, Soares R, Gama M. 2011. Studies on the hemocompatibility of bacterial cellulose. J Biomed Mater Res A 98A:554–66.

Bekyarova E, Ni YC, Malarkery EB, Montana V, McWilliams JL, Haddon RC, Parpura V. 2005. Applications of carbon nanotubes in biotechnology and biomedicine. J Biomed Nanotechnol 1:3–17.

Bleek K, Taubert A. 2013. New developments in polymer-controlled, bioinspired calcium phosphate mineralization from aqueous solution. Acta Biomater 9:6283–321.

Bisht S, Bhakta G, Mitra S, Maitra A. 2005. pDNA loaded calcium phosphate nanoparticles: highly efficient non-viral vector for gene delivery. Int J Pharm 288:157–68.

Cai Y, Yao J. 2010. Effect of proteins on the synthesis and assembly of calcium phosphate nanomaterials. Nanoscale 2:1842–8.

Chen F, Huang P, Zhu YJ, Wu J, Cui DX. 2012. Multifunctional Eu3þ/Gd3þ dual-doped calcium phosphate vesicle-like nanospheres for sustained drug release and imaging. Biomaterials 33:6447–55.

Chen F, Zhu YJ, Zhang KH, Wu J, Wang KW, Tang QL, Mo XM. 2011. Europium-doped amorphous calcium phosphate porous nanospheres: preparation and application as luminescent drug carriers. Nanoscale Res Lett 6:67.

Chen X, Park R, Hou Y, Khankaldyyan V, Gonzales-Gomez I, Tohme M, et al. 2004. MicroPET imaging of brain tumor angiogenesis with 18F-labeled PEGylated RGD peptide. Eur J Nucl Med Mol Imaging 31:1081–9.

Corbin IR, Chen J, Cao WG, Li H, Lund-Katz S, Zheng G. 2007. Enhanced cancer-trageted delivery using engineered high-density lipoprotein-based nanocarriers. J Biomed Nanotechnol 3:367–76.

Chow LC, Takagi S. 2001. A natural bone cement – a laboratory novelty led to the development of revolutionary new biomaterials. J Res Natl Inst Stand Technol 106:1029–33.

Cun DM, Jensen LB, Nielsen HM, Moghimi M, Foged C. 2008. Polymeric nanocarriers for siRNA delivery: challenges and future propects. J Biomed Nanotechnol 4:258–75.

Deng J, Yu L, Liu C, Yu K, Shi X, Yeung LWY, et al. 2009. Hexabromocyclododecane-induced developmental toxicity and apoptosis in zebrafish embryos. Aquat Toxicol 93:29–36.

Fujiwara M, Shiokawa K, Morigaki K, Tatsu Y, Nakahara Y. 2008. Calcium phosphate composite materials including inorganic powders, BSA or duplex DNA prepared by W/O/W interfacial reaction method. Mater Sci Eng C 28:280–8.

Ginebra MP, Canal C, Espanol M, Pastorino D, Montufar EB. 2012. Calcium phosphate cements as drug delivery materials. Adv Drug Deliv Rev 64:1090–110.

Han MH, Chen J, Wang J, Chen SL, Wang XT. 2005. Blood compatibility of polyamidoamine dendrimers and erythrocyte protein. J Biomed Nanotechnol 6:82–92.

Kim WJ, Yockman JW, Lee M, Jeong JH, Kim YH, Kim SW. 2005. Soluble Flt-1 gene delivery using PEI-g-PEG-RGD conjugate for anti-angiogenesis. J Control Release 106:224–34.

Malafaya PB, Silva GA, Reis RL. 2007. Natural-origin polymers as carriers and scaffolds for biomolecules and cell delivery in tissue engineering applications. Adv Drug Deliv Rev 59:207–33.

McGinley EL, Coleman DC, Moran GP, Fleming GJP. 2011. Effects of surface finishing conditions on the biocompatibility of a nickel-chromium dental casting alloy. Dent Mater 27:637–50.

Morishige T, Yoshioka Y, Tanabe A, Yao X, Tsunoda S, Tsutsumi Y, et al. 2010. Titanium dioxide induces different levels of IL-1β production dependent on its particle characteristics through caspase-1 activation mediated by reactive oxygen species and cathepsin B. Biochem Biophys Res Commun 392:160–5.

Muzzarelli RAA, Guerrieri M, Goteri G, Muzzarelli C, Armeni T, Ghiselli R, Cornelissen M. 2005. The biocompatibility of dibutyryl chitinin the context of wound dressings. Biomaterials 26: 5844–54.

Mukesh U, Kulkarni V, Tushar R, Murthy RSR. 2009. Methotrexate loaded self stabilized calcium phosphate nanoparticles: a novel inorganic carrier for intracellular drug delivery. J Biomed Nanotechnol 5:99–105.

Nie Y, Duan Y, Zhang Z. 2007. Evaluation of blood compatibility of surface modification treated poly(D,L-lactic and glycolic acid)with mPEG block copolymer. J Biomed Eng 24:336–9.

Ng SX, Guo J, Ma J, Chye S, Loo J. 2010. Synthesis of high surface area mesostructured calcium phosphate particles. Acta Biomater 6: 3772–81.

Qi C, Zhu YJ, Lu BQ, Zhao XY, Zhao J, Chen F. 2012. Hydroxyapatite nanosheet-assembled porous hollow microspheres: DNA-templated hydrothermal synthesis, drug delivery and protein adsorption. J Mater Chem 22:22642–50.

Olton DYE, Close JM, Sfeir CS, Kumta PN. 2011. Intracellular trafficking pathways involved in the gene transfer of nano-structured calcium phosphate-DNA particles. Biomaterials 32:7662–70.

Salah R, Michaud P, Mati F, Harrat Z, Lounici H, Abdi N, et al. 2013. Anticancer activity of chemically prepared shrimp low molecular weight chitin evaluation with the human monocyte leukaemia cell line, THP-1. Int J Biol Macromol 52:333–9.

Sangeetha J, Thomas S, Arutchelvi J, Doble M, Philip J. 2013. Functionalization of iron oxide nanoparticles with biosurfactants and biocompatibility studies. J Biomed Nanotechnol 9: 751–64.

Schiffelers RM, Mixson AJ, Ansari AM, Fens MHAM, Tang Q, Zhou Q, et al. 2005. Transporting silence: design of

carriers for siRNA to angiogenic endothelium. J Control Release 109:5–14.

Shen SF, Zhao HW, Huang CZ, Wu LP. 2012. Higher-order structures assembly of gold nanorods caused by captopril in high ionic strength solutions. J Biomed Nanotechnol 6:66–72.

Sun Y, Chen XY, Zhu YJ, Liu PF, Zhu MJ, Duan YR. 2012. Synthesis of calcium phosphate/GPC-mPEG hybrid porous nanospheres for drug delivery to overcome multidrug resistance in human breast cancer. J Mater Chem 22:5128–513.

Wang KW, Zhou LZ, Sun Y, Wu GJ, Gu HC, Duan YR, et al. 2010a. Calcium phosphate/PLGA-mPEG hybrid porous nanospheres: a promising vector with ultrahigh gene loading and transfection efficiency. J Mater Chem 20:1161–6.

Wang KW, Zhu YJ, Chen XY, Zhai WY, Wang Q, Chen F, et al. 2010b. Flower-like hierarchically nanostructured hydroxyapatite hollow spheres: facile preparation and application in anticancer drug cellular delivery. Chem Asian J 5:2477–82.

Wu J, Zhu YJ, Chen F, Zhao XY, Zhao J, Qi C. 2013. Amorphous calcium silicate hydrate/block copolymer hybrid nanoparticles: synthesis and application as drug carriers. Dalton Trans 42:7032–40.

Wang Q, Gong T, Sun X, Zhang Z. 2011. Structural characterization of novel phospholipid lipid nanoparticles for controlled drug delivery. Colloids Surf. B Biointerfaces 84:406–12.

Wang QZ, Chen XG, Li ZX, Wang S, Liu CS, Meng XH, et al. 2008. Preparation and blood coagulation evaluation of chitosan microspheres. J Mater Sci: Mater Med 19:1371–7.